UNDERSTANDING IMBIBITION DATA IN COMPLEX CARBONATE ROCK TYPES

Moustafa Dernaika[1], Zubair Kalam[2], Svein Skjaeveland[3]
[1]Ingrain Inc.-Abu Dhabi, [2]ADCO, [3]University of Stavanger

This paper was prepared for presentation at the International Symposium of the Society of Core Analysts held in Avignon, France, 8-11 September, 2014

ABSTRACT
Carbonate rocks are complex in their structures and pore geometries and often exhibit a real problem in their classification and behavior. Many petrophysical and fluid flow properties remain unexplained and perhaps uncertain because of improper characterization of the reservoir rock.

In this research, carbonate rock types were defined from thin-sections based on the structure of the rock together with its pore types. The rock type classifications were improved by incorporating pore-throat size distribution and poro-perm information, and high resolution plug CT images. This would lead to a robust rock typing scheme that should facilitate the understanding of heterogeneity effects on reservoir flow properties.

Laboratory-measured imbibition relative permeability (Kr) data were determined on reservoir core samples in two "mixed-wet" carbonate fields from the Middle East region. The Kr curves were explained based on the identified rock types and gave consistent trends. The Kr curves were fitted with Corey exponents, and yielded high "no" and low "nw" for the higher permeability samples, which may be wrongly interpreted as more oil-wet rocks compared to the lower permeability samples. The variations in Kr curves with the different rock types were argued to be the result of different rock structures and pore geometries that control pore accessibility and surface area. The obtained Krw and Kro data from steady state experiments are not abundant in the literature and hence should serve as an important piece of information in mixed-wet carbonate reservoirs with varying rock types.

INTRODUCTION
Core laboratory data can have a major impact on the reservoir modeling process but often yield unrepresentative measurements that raise questions about the effectiveness of the core data in the reservoir model and its calibration. This is partly related to the lack of understanding of the reservoir rock types, hence the obtained SCAL data would be left unexplained and often no attempt would be possible to link the macroscopic measurements to fundamental microscopic properties and geological heterogeneities within the reservoir.

In this research work, experimental relative permeability measurements were investigated in two different fields in complex "mixed-wet" carbonate reservoirs. Imbibition relative permeability (Kr) curves were determined by the steady state equilibrium fractional flow method at full reservoir conditions using live fluids and in-situ saturation monitoring. The core plug samples were selected to represent main rock types in the reservoirs based on geological and petrophysical data. Large variations were seen in the Kr curves among the different rock types that would generally be referred to wettability and/or heterogeneity considerations without much explanation or understanding of the underlying reasons. It was found out that rock texture and pore geometry are two important parameters in carbonate porous media that are necessary to understand in order to explain the macroscopic measurements and to link them to proper rock types in the core.

EXPERIMENTAL MEASUREMENTS

A total of sixteen 1.5" diameter core plugs were chosen based on detailed thin-section descriptions and mercury injection. All the 16 samples underwent imbibition Kr experiments at full reservoir conditions. Table 1 gives representative plug data from six samples which represent the main rock type variations in two different fields (A &B) in Abu Dhabi. Figure 1 presents the rock characterization of the three samples (rock types) from field A. Each sample is classified based on poro-perm, thin-section photomicrograph, mercury-derived pore-throat size distribution (PTSD), and X-ray CT imaging. The CT image was cropped from the middle slice along the sample length. Figure 2 shows similar information from three main rock types in field B.

The individual plugs were thoroughly cleaned by flow through techniques to render the rocks water wet. Each core plug sample was saturated with 100% simulated formation water and was de-saturated to irreducible brine saturation (Swi) using the porous plate method. Prior to the steady-state imbibition Kr measurements, each core sample was aged for three weeks in live fluids at full reservoir conditions of temperature, overburden stress and pore pressure. This aging condition is believed to render the rocks mixed-wet to oil-wet for representative wettability condition. At the end of the wettability restoration, the sample effective oil permeability (Ko(Swi)) was measured, and was used as the reference (base) permeability to define relative permeability. Capillary pressure experiments by porous plate and centrifuge were conducted on similar rock types and showed no spontaneous imbibition. This confirmed the wettability state (mixed-wet to oil-wet) of all the investigated samples in this study.

Injection at fractional flow rates was continued until the pressure and production had stabilized, before altering the fractional flow rate to the next predetermined step. High rate bump flood was performed at the end of imbibition to counter capillary end effects. Numerical simulation was performed on the core flood experiments using Sendra^{TM}, which showed good match between simulated curves and experimental data. Details on the numerical simulations and experimental procedures may be found in [1].

RESULTS AND DISCUSSIONS

Figure 3 shows the poroperm data from the 6 samples. Calcitic samples (1, 2 & 3) from field A have almost similar porosity values with varying permeability. The permeability seems to increase with larger grain size and larger pores. These can be seen in the corresponding thin-sections and MICP curves in Figure 1. The rock types in field B also show higher permeability with bigger grain size (more grainy rock type). Sample #4 is the only dolomitic sample, which has porosity in the lower range. The X-ray CT images were obtained at 40microns per voxel and show the complex vuggy nature of sample #1 and #2 from field A.

Figure 5 presents the imbibition Kro and Krw curves from the different six rock types in field A and field B. Table 1 records the fitting Corey exponents together with Swi, Sor and Krw_{max}. Figure 4 depicts the variation of Corey exponents with permeability. The following observations can be made:

1. Consistent Kr trend with permeability (rock type)
2. Higher permeability yields higher Krw curves but lower Kro curves
3. Variation of Krw curves is greater than variation of Kro curves (see also figure 4)
4. Higher permeability tends to yield higher Krw_{max}
5. Higher permeability samples (more heterogeneous) give higher average Sor
6. The inlet Sor (at the injection end) is lower than average Sor (due to Pc end effect)
7. Higher permeability plugs show bigger difference between average Sor and inlet Sor
8. Higher permeability samples give higher “no” and lower “nw” exponents

One may be tempted to explain the variations in the Kr curves based on wettability variations among the different samples [2,3] but this may lead to wrong conclusions. The variation in Corey exponents should not be interpreted based on wettability because all those samples showed, more or less, similar wettability characteristics from Pc measurements. The variation in Corey exponents must be the result of the different rock types (rock structure and pore geometry). It should also be mentioned here that the effect of wettability on the relative permeability end points is subject for discussions, and the ability to explore wettability from Kr curves is questioned by several researchers [4], especially for mixed wettability systems.

The increase in Krw with higher permeability (bigger pores/grains) should be related to better pore accessibility and smaller surface area in such porous systems. On the other hand, the decrease in Kro with higher permeability may be due to the quick production of oil from the large pores in the system that leaves less oil to move in the bigger pores.

The variation of Krw curves with different rock types is larger than that of Kro because the advancing water in imbibition would have different behavior than the defending oil. This is also true and has indeed been observed in primary drainage Kr experiments where Kro (oil being the advancing fluid) experienced more variations than Krw [1]. The advancing fluid would be more influenced by pore geometry than the defending fluid. In this perspective, the invading fluid is entering into new locations in the pore system and

should be controlled by available capillaries among different rock types, whereas the defending fluid (oil in this case) escapes from the system with a continuous phase.

The more heterogeneous rock types (with higher permeabilities) have wider PTSD and more complex geometries that could lead to higher average residual oil saturations (Sor) values at the end of the core water flood. The trapped oil would have been bypassed by the water due to large variations in the pore sizes and possible porosity channels. Large part of this bypassed oil was recovered by the high rate bump flood. Better estimation of Sor was obtained from in-situ saturation profiles at the inlet of the core (Table 1). The most accurate Sor would of course be determined from proper imbibition capillary pressure experiments and in this case was found to be very close to the predicted Sor at the injection end of the core flood.

CONCLUSION

Complex carbonate rock types were identified based on geological and petrophysical variations. More grainy (heterogeneous) samples are characterised by higher permeability, while smaller permeability samples are less heterogeneous with smaller grain/pore sizes. Imbibition Kr curves showed large variations among the different rock types. The curves were fitted with Corey exponents and showed large variations that should not be interpreted based on wettability considerations. The Kr curves were determined from core-flood steady-state equilibrium fractional flow rate method at full reservoir conditions, which enabled the derivation of both Kro and Krw curves.

1. Both Krw and Kro vary with rock type: Krw increases with permeability while Kro decreases. Pore accessibility and surface area may be the main cause of this variation.
2. Krw varies more with different rock types (permeability) than does Kro in imbibition.
3. More heterogeneous (higher permeability) samples experienced greater Pc end effects
4. Higher permeability samples give higher “no” and lower “nw” exponents (this is not the effect of wettability)

ACKNOWLEDGEMENTS

The authors wish to acknowledge ADCO and ADNOC management for the permission to publish the results of this research study.

REFERENCES

1. Dernaika, M.R., Basioni, M., Dawoud, A., Kalam, M.Z., and Skjæveland, S.M. “Variations in Bounding and Scanning Relative Permeability Curves with Different Carbonate Rock Types” *J. Res. Eval. & Eng.* (August 2013).
2. Masalmeh, S.K.: “Experimental Measurements of Capillary Pressure and Relative Permeability Hysteresis” SCA 2001-23 presented at the SCA 2001 conference, Edinburgh, September (2001).
3. Honarpour, M., Koederitz, L., and Harvey, A.H., Relative Permeability of Petroleum Reservoirs, CRC Press Inc, Boca Raton, 1987.
4. Morrow, N.R., Wettability and Its Effect on Oil Recovery, JPT, 1476-84, Dec. 1990.

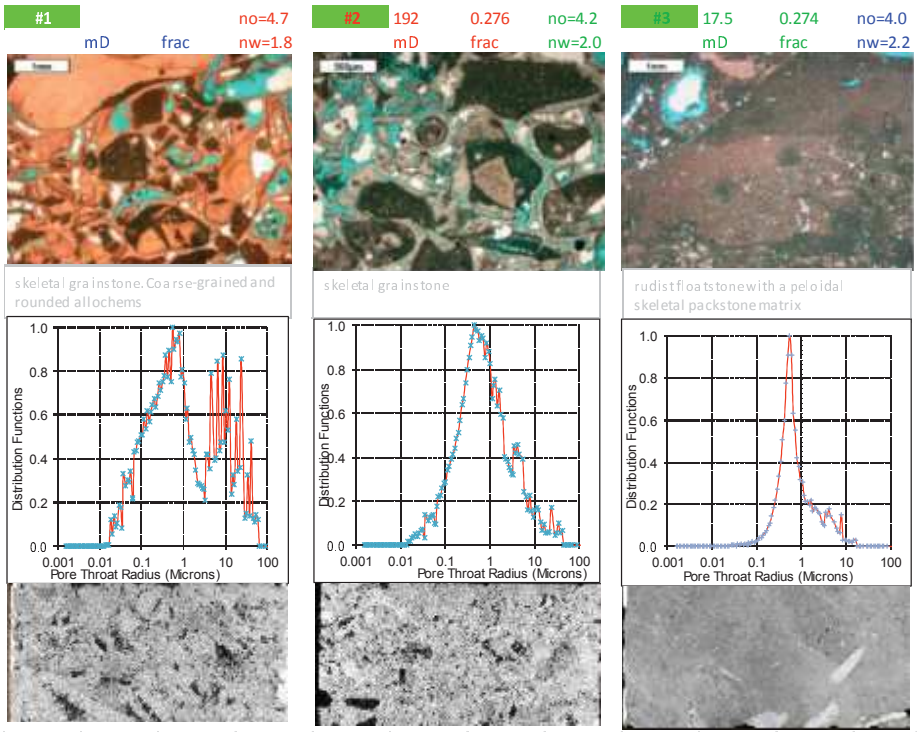

Figure 1 Rock Characterisation for the main rock types in field A. Each sample is shown with poro perm data, Corey exponents, thin-section photomicrograph, mercury-derived PTSD, and X-ray CT image.

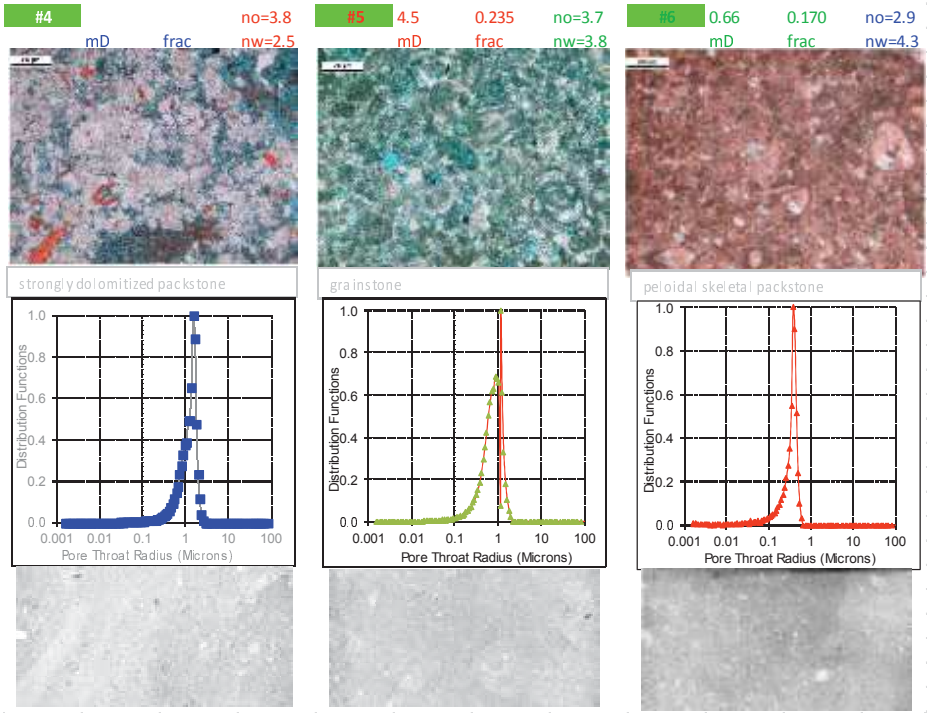

Figure 2 Rock Characterisation for the main rock types in field B. Each sample is shown with poroperm data, Corey-exponents, thin-section photomicrograph, mercury-derived PTSD, and X-ray CT image.

Table 1 Reservoir properties from all six samples (field A & B)

Field	SN	Porosity (frac)	Kw (mD)	Ko(Swi) (mD)	Swi (frac)	nw	no	Average Sor (PV)	Sor (PV) at inlet	Krwmax (Av Sor)
A	1	0.270	392	490	0.078	1.8	4.7	0.297	0.200	0.749
A	2	0.276	198	192	0.090	2	4.2	0.312	0.200	0.758
A	3	0.274	21	17.5	0.134	2.2	4.0	0.208	0.150	0.588
B	4	0.181	21	15.1	0.178	2.5	3.8	0.209	0.201	0.654
B	5	0.235	7.0	4.5	0.067	3.8	3.7	0.080	0.067	0.820
B	6	0.170	0.81	0.66	0.094	4.3	2.9	0.207	0.186	0.236

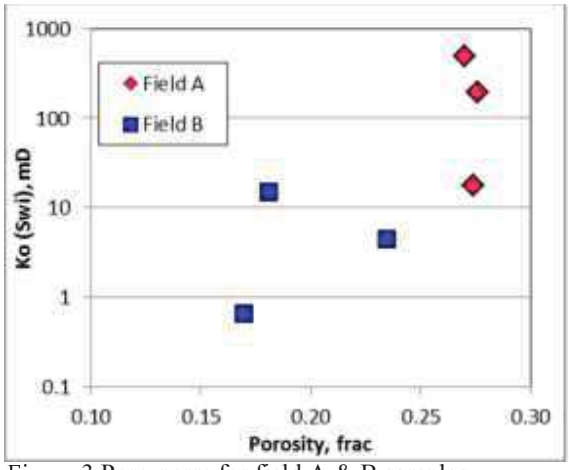

Figure 3 Poro-perm for field A & B samples

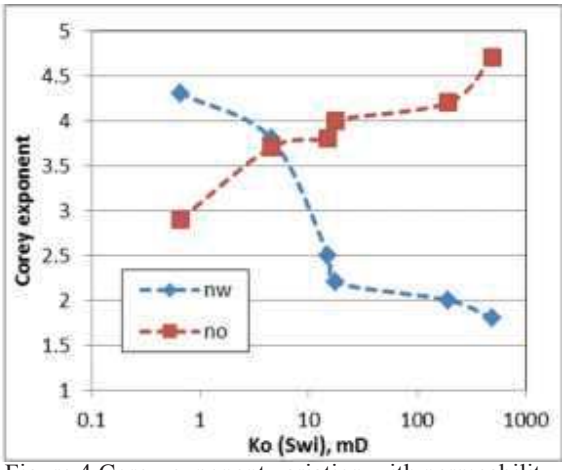

Figure 4 Corey-exponent variation with permeability

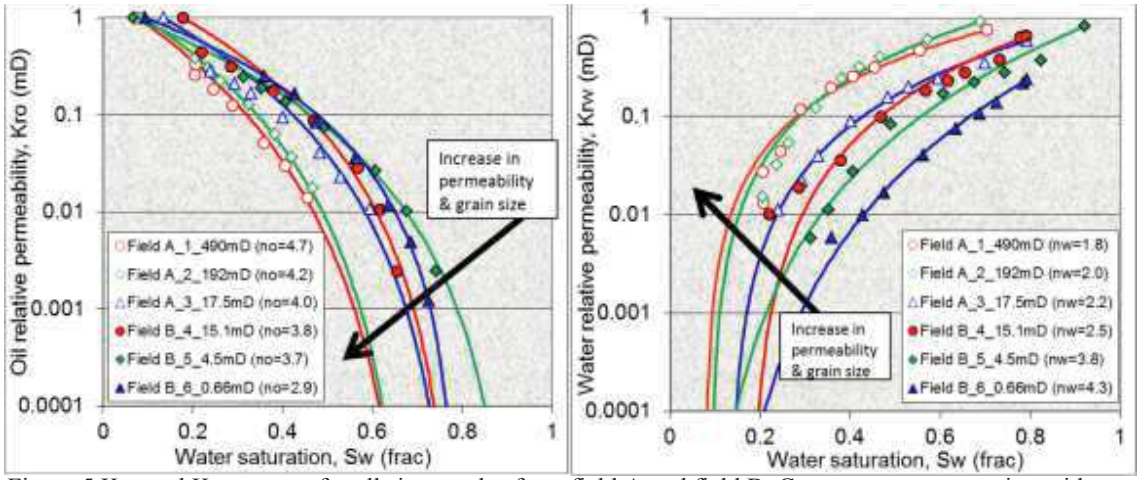

Figure 5 Kro and Krw curves for all six samples from field A and field B. Corey exponents varying with different rock types and permeability.